Communications Research Centre Canada
Centre de recherches sur les communications Canada
An Agency of Industry Canada
Un organisme d'Industrie Canada

Mobile Transmitters Tracking Using Geodetic Models with Multiple Receivers

Ming-Wang Tu

March 2, 2004

Communications Research Centre Canada
Ottawa, Canada

Canada

CENTRE DE RECHERCHES SUR LES COMMUNICATIONS RESEARCH CENTRE

Background

- This study uses AOA method for spectrum surveillance applications (e.g. CRC's Spectrum Explorer).
- A wideband scanning device is needed since various signals may occupy a wide frequency band.
- Basic preliminary channel usage info usually includes multiple (channel#, SNR, AOA, AOA ISD) for each scan. Thus, a pre-ssing (first-step) procedure (signal detection, type dentification, direction finding) is needed.
  scans, the basic preliminary channel usage info is
  cessed by a (second-step) procedure to get the overall channel usage

Goal

- Based on the overall channel usage report (active channel#, EST_AOA, EST_SD) from each RX to various TXs, develop a set of simple algorithms (third-step procedure) to track mobile TXs efficiently.

Approach

- Use two geodetic models (Spherical and WGS84) with two/three-RX (2R/3R) fixing to process the overall channel usage report data from each RX to various TXs.

Spherical Model

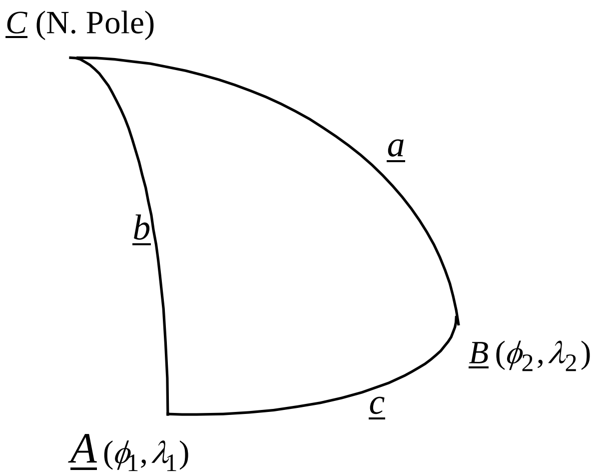

$$\sin \underline{A} / \sin \underline{a} = \sin \underline{B} / \sin \underline{b} = \sin \underline{C} / \sin \underline{c} \qquad (1)$$

$$\cos \underline{C} = -\cos \underline{B} \cos \underline{A} + \sin \underline{B} \sin \underline{A} \cos \underline{c} \qquad (2)$$

$$\sin \; Az \; / \cos \; \phi_2 = \sin(\lambda_2 - \lambda_1) / \sin \; \underline{c} \qquad (3)$$

$$\cos \underline{c} = \sin \phi_1 \sin \phi_2 + \cos \phi_1 \cos \phi_2 \cos(\lambda_2 - \lambda_1) \qquad (4)$$

$$\cos Az = [\cos \phi_1 \sin \phi_2 - \sin \phi_1 \cos \phi_2 \cos(\lambda_2 - \lambda_1)] / \sin \underline{c} \qquad (5)$$

$$\phi_2 = \arcsin(\sin \phi_1 \cos \underline{c} + \cos \phi_1 \sin \underline{c} \cos Az) \qquad (6)$$

- (ϕ, λ) = (latitude, longitude). Angle $\underline{A}$ is the azimuth Az east of north (clockwise) which point $\underline{B}$ bears to point $\underline{A}$.

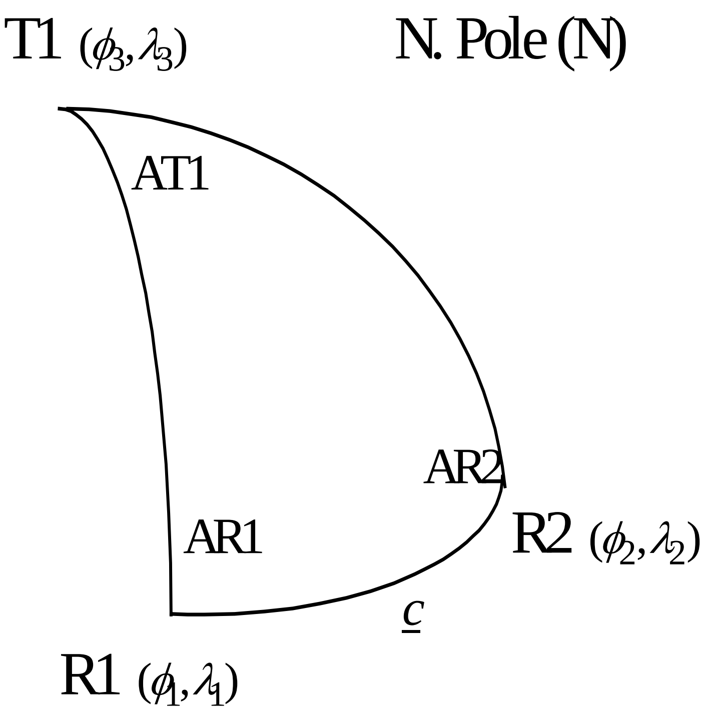

1. Given (ϕ_1,λ_1) and (ϕ_2,λ_2), (4)=>S_R1R2_Spherical (=$\underline{c}R$).
2. (3),(5)=>(A12,A21) (tri R1-R2-N).

   (AR1,AR2)=(AOA1,AOA2)-(A12,A21).

   | | |

   (tri R1-R2-T1) (tri R1,2-N-T1) (tri R1-R2-N)
3. (2)=>AT1, (1)=>S_R1T1_Spherical.
4. Given S_R1T1_Spherical and AOA1, (4),(6)=> (ϕ_3,λ_3).
5. Repeat for multiple AOA1/2 sets for multiple TXs.
6. Extend to 3R fixing by processing 2 RXs at a time.

WGS84 Model

$$S \sin Az = Nl \cos\phi[1-(l\sin\phi)^2/24+(1+\eta^2-9\eta^2t^2)b^2/24V^4] \quad (7)$$

$$S\cos Az = Nb'\cos(l/2)[1+(1-2\eta^2)(l\cos\phi)^2/24+\eta^2(1-t^2)b'^2/8V^4] \quad (8)$$

$$\Delta Az = l\sin\phi[1+(1+\eta^2)(l\cos\phi)^2/12+(3+8\eta^2)b^2/24V^4] \quad (9)$$

$$l = S\sin Az[1+(l\sin\phi)^2/24-(1+\eta^2-9\eta^2t^2)b^2/24V^4]/N\cos\phi \quad (10)$$

$$b' = S\cos Az[1-(1-2\eta^2)(l\cos\phi)^2/24-\eta^2(1-t^2)b'^2/8V^4]/N\cos(l/2) \quad (11)$$

$$C_m(\phi) = R(1-e^2\sin^2\phi)^{3/2}/[a(1-e^2)] \quad (12) \qquad C_p(\phi) = R(1-e^2\sin^2\phi)^{1/2}/a \quad (13)$$

$$C_{sp\_ellips} = [\sqrt{C_m^2(\phi_1)+C_p^2(\phi_1)}+\sqrt{C_m^2(\phi_2)+C_p^2(\phi_2)}]/2 \quad (14)$$

$$= \quad (15)$$

$\phi = (\phi_1+\phi_2)/2, l = \lambda_2-\lambda_1, b = \phi_2-\phi_1, t = \tan\phi, \eta = e'\cos\phi,$

$e'^2 = (a^2-b^2)/b^2, V^2 = 1+\eta^2, f = (a-b)/a, c = a^2/b,$

$N = a/\sqrt{1-f(2-f)\sin^2\phi}, V = c/N, b' = b/V^2,$

- a (=6378.137 km): semimajor axis (equatorial radius) of earth;
  b: semiminor axis (polar radius) of earth; f (=1/298.257223563): flattening;
  e': second eccentricity; $e = (1 - b^2 / a^2)^{1/2}$: eccentricity of the ellipsoid.
- $C_m(\phi) / C_p(\phi)$: ratio for the length of a radian of latitude/longitude along a meridian/parallel on the sphere to that on the ellipsoid.

1. Given and , (7) and (8)=>(S_R1R2_WGS84),

(ϕ_1, λ_1) (ϕ_2, λ_2)

$\underline{c} = S_{\_R1R2\_Spherical} / R$

(ϕ_3, λ_3).

2R Fixing

- The 2R Fixing has been mentioned in both geodetic models. In general, for both models, the procedure is as follows:

1. Given (ϕ_1,λ_1) and (ϕ_2,λ_2) for R1 and R2, find S_R1R2_Spherical.
2. Find (A12, A21). (AR1,AR2)=(AOA1,AOA2)-(A12,A21).
3. Use (2) to find AT1. Use (1) to find S_R1T1_Spherical, (15)=> S_R1T1_WGS84 if for WGS84 model.
4. Given S_R1T1_Spherical/WGS84 and AOA1, find (ϕ_3,λ_3).
5. Repeat for multiple AOA1/2 sets for multiple TXs.

3R Fixing

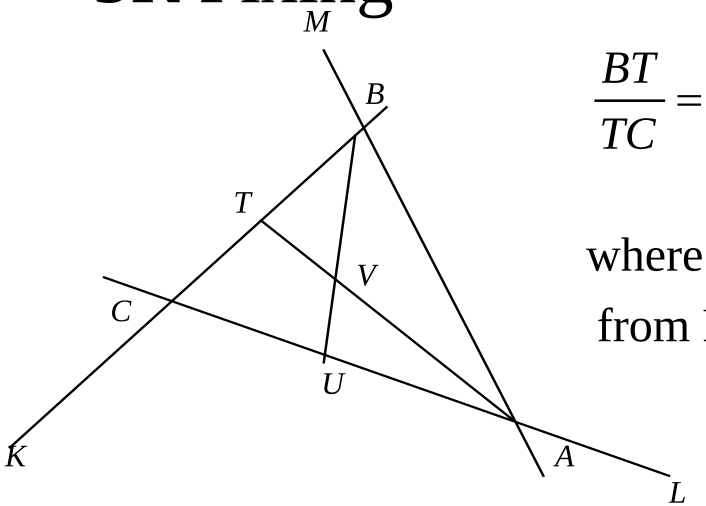

$$\frac{BT}{TC}=\frac{D_M^2\sigma_{\psi M}^2\sin^2 BCA}{D_L^2\sigma_{\psi L}^2\sin^2 ABC},\frac{CU}{UA}=\frac{D_K^2\sigma_{\psi K}^2\sin^2 CAB}{D_M^2\sigma_{\psi M}^2\sin^2 BCA}\quad(16,17)$$

where $D_K = KC, D_L = LA, D_M = MB.$ $\sigma_{\psi J}$ is the AOA SD from RX *J* (=*K*,*L*,*M*). By Menelaus' Theorem,

$CA\times VU\times BT = UA\times BV\times TC$, then

$$\frac{BV}{VU}=\frac{BT}{TC}\times\frac{CA}{UA}=\frac{BT}{TC}\times(1+\frac{CU}{UA})\quad(18)$$

- *K*, *L* and *M* represent the RXs and *A*, *B*, *C* the corresponding corners of a triangle. The best estimated location of the TX is at *V*.
- For various mobile TXs, we can repeat the 2R fixing procedure for e for multiple AOA1/2/3 sets for the 3R fixing to find the sets of (*A*, *B*, en, (16), (17) and (18) can be used to find the *V*s to track those mobile TXs.

e mobile TXs.

Confidence Ellipse (CE)

$$\frac{X^2}{r^2}+\frac{Y^2}{s^2}=-2\log_{\varepsilon}(1-P),\qquad \frac{1}{r^2}=2\kappa-\nu\tan\varphi,\qquad \frac{1}{s^2}=2\mu+\nu\tan\varphi,$$

$$\kappa=\sum_J\frac{\sin^2\theta_J}{\sigma_{\psi J}^2D_J^2},\qquad \mu=\sum_J\frac{\cos^2\theta_J}{\sigma_{\psi J}^2D_J^2},\qquad \nu=\sum_J\frac{\sin\theta_J\cos\theta_J}{\sigma_{\psi J}^2D_J^2},\qquad \tan2\varphi=-\frac{2\nu}{\kappa-\mu},$$

θ_J : AOA from RX J.

φ : X, Y rotating angle relative to the coordinates x, y.

- The CE with probability P is the probability that the V of a mobile TX will lie within the area bounded by an elliptical contour with semimajor axis r and semiminor axis s.
- $(r, s, \kappa, \mu, \nu, \varphi)$ and the CE vary as the AOA varies. The CE can be applied to both the 2R and 3R fixings.

Simulated Results

- 3 RXs located at Mont Royal (R1) and St-Remi (R2) in Quebec, Canada and a dummy location (R3) were simulated with (ϕ, λ) set

d with $(45.50'', -72.[illegible]9'')$ set, $(45.28'', -72.33''), (45.43'', -72.68''),$

als to respectively.

vely.

with 25-dB EST_SNR were simulated. AOAi_Tj represents

azimuth from RX i to TX j.

5-dB SNR, AOA SD ~ 2 dgs.

25-dB SNR, |*N*(AOA_true, 1&2-dg SD)| and |*N*(0, 1&2-dg SD)| were

1&2-dg SD)| were used as the AOA and AOA SD models,

&2-dg SD)| were used as the AOA and AOA SD models, respectively,

- For the 2R/3R fixing, (R1, R2)/(R1, R2, R3) and (AOA1, AOA2)/(AOA1, AOA2, AOA3) were used.
- 20 snapshots of simulated data were generated for each case using the sets of the AOAi_Tj with its AOA SD.
- The following values were calculated among the 20 snapshots:

(*r_max*, *s_max*): maximum of *r*s, *s*s, and its CE.

*Vavg*_Tj: averaged *V*_Tjs.

True_Tj: The true location of Tj (calculated by using zero AOA SDs).

Rec_AOAi_Tj: recalculated AOAi_Tj (azimuth from Ri to *Vavg*_Tj).

Er_AOAi_Tj: AOAi_Tj error (=Rec_AOAi_Tj–AOAi_Tj_true).

RMSD_Tj: Root-mean-square distance (between *V*_Tjs and True_Tj).

AREACE_Tj: CE area.

- Both the Spherical and WGS84 models were used. For the cases of mobile TXs, Er_AOAi_Tj(1,2), True_Tj(1,2), *Vavg*_Tj(1,2), (*r_max*, *s_max*)_Tj(1,2), RMSD_Tj(1,2) and AREACE_Tj(1,2) were calculated.

- Simulated Test1 Scenario: Motionless T1 for a 2R fixing, (AOA1, AOA2)=(225,315) with (I): 1-dg AOA SD and *P*=50% CE; (II): 1-dg AOA SD and *P*=99% CE; (III): 2-dg AOA SD and *P*=99% CE.

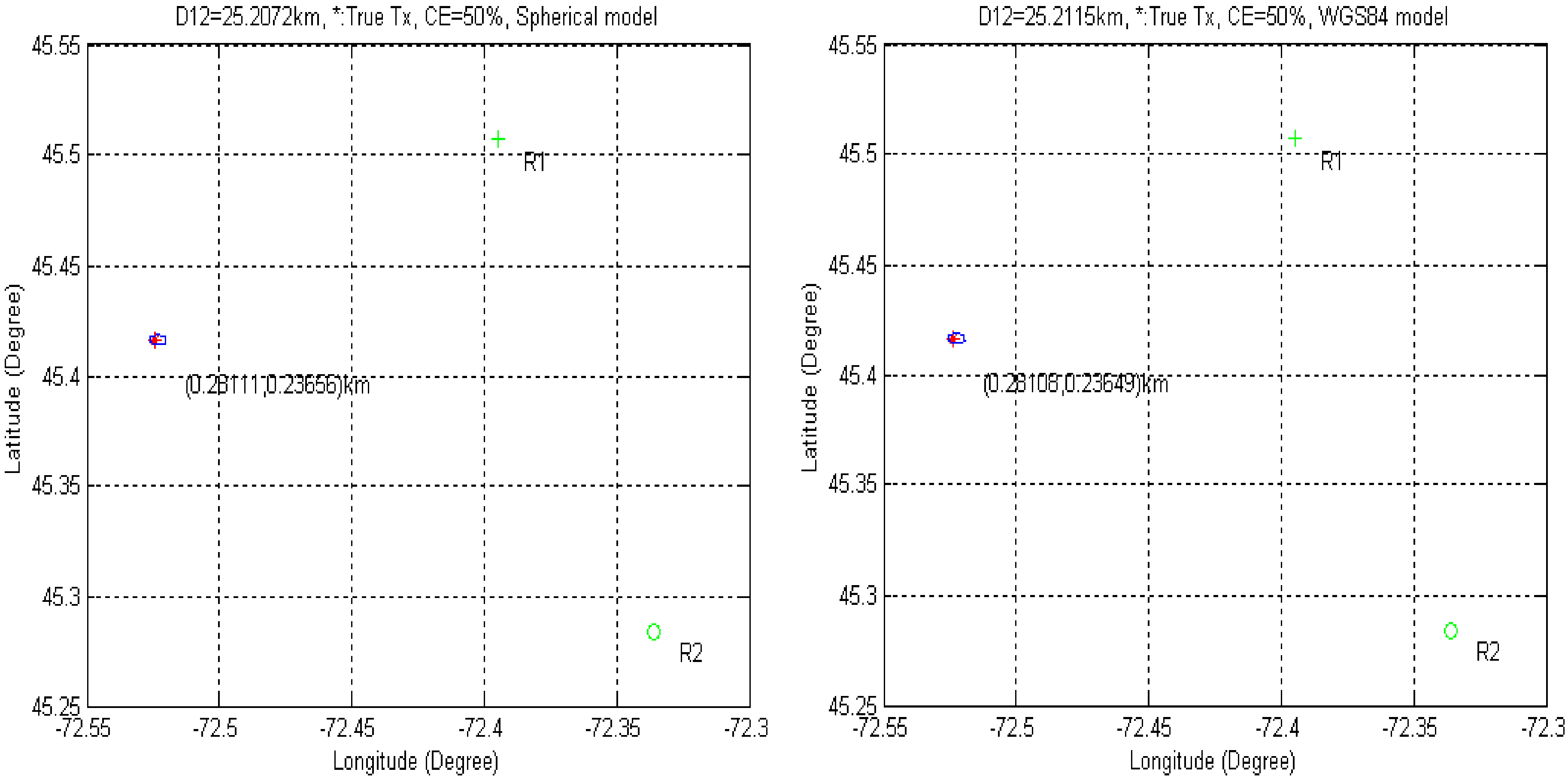

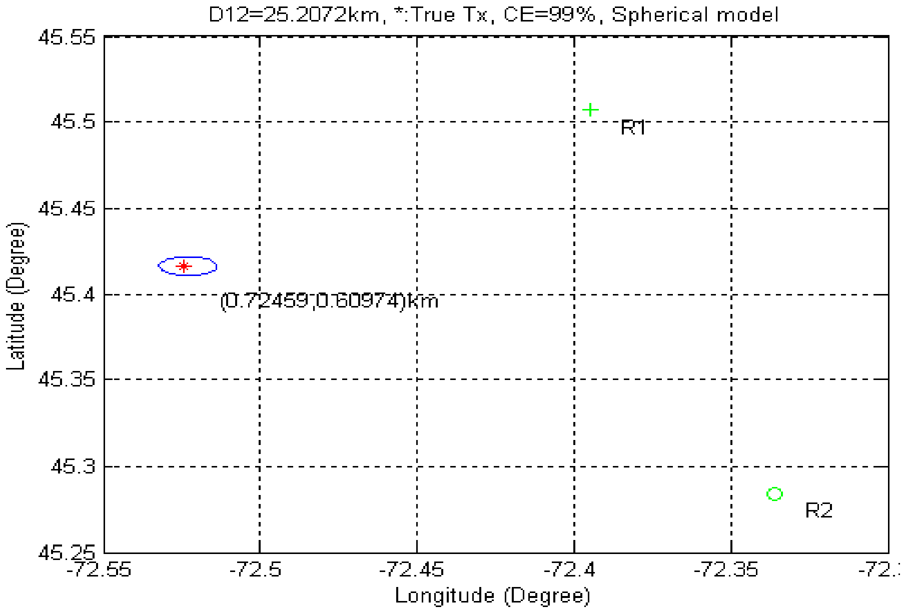
D12=25.2072km, *:True Tx, CE=99%, Spherical model
R1
R2
(0.72459,0.60974)km
Latitude (Degree)
Longitude (Degree)
45.55
45.5
45.45
45.4
45.35
45.3
45.25
-72.55
-72.5
-72.45
-72.4
-72.35

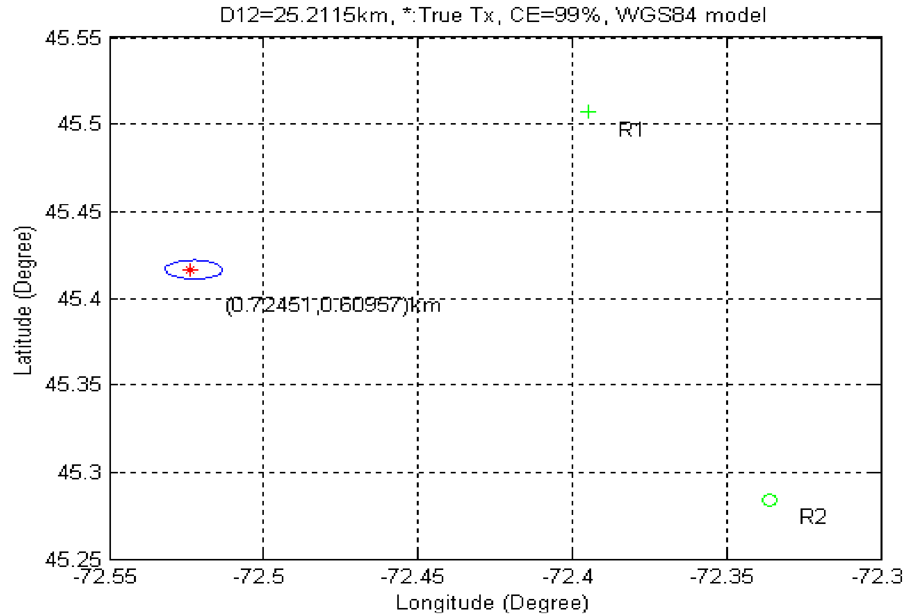
D12=25.2115km, *:True Tx, CE=99%, WGS84 model
R1
R2
(0.72451,0.60957)km
Latitude (Degree)
Longitude (Degree)
45.55
45.5
45.45
45.4
45.35
45.3
45.25
-72.55
-72.5
-72.45
-72.4
-72.35
-72.3

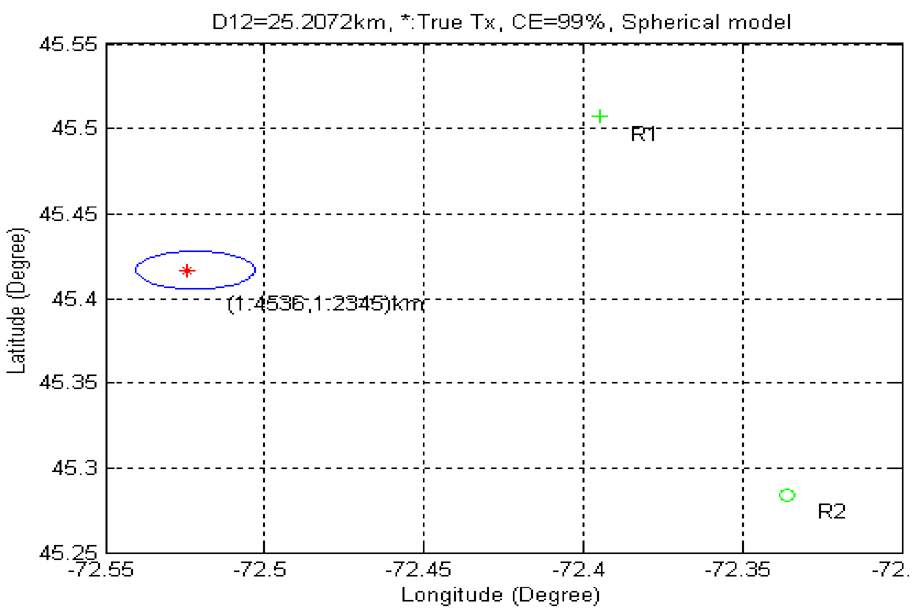
D12=25.2072km, *:True Tx, CE=99%, Spherical model
R1
R2
(1.4536,1.2345)km
Latitude (Degree)
Longitude (Degree)
45.55
45.5
45.45
45.4
45.35
45.3
45.25
-72.55
-72.5
-72.45
-72.4
-72.35

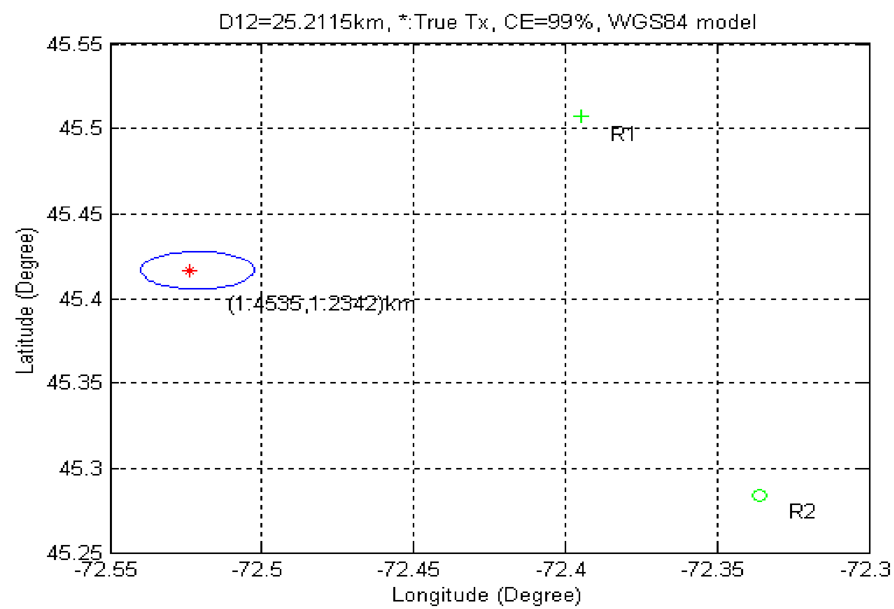
D12=25.2115km, *:True Tx, CE=99%, WGS84 model
R1
R2
(1.4535,1.2342)km
Latitude (Degree)
Longitude (Degree)
45.55
45.5
45.45
45.4
45.35
45.3
45.25
-72.55
-72.5
-72.45
-72.4
-72.35
-72.3

- Simulated Test2 Scenario: Mobile T1&T2 for a 2R fixing with 2-dg AOA SD and *P*=99% CE. AOA1,2_T1(1,2)=(225°,228°),(315°,318°), AOA1,2_T2(1,2)=(235°,238°),(325°,328°).

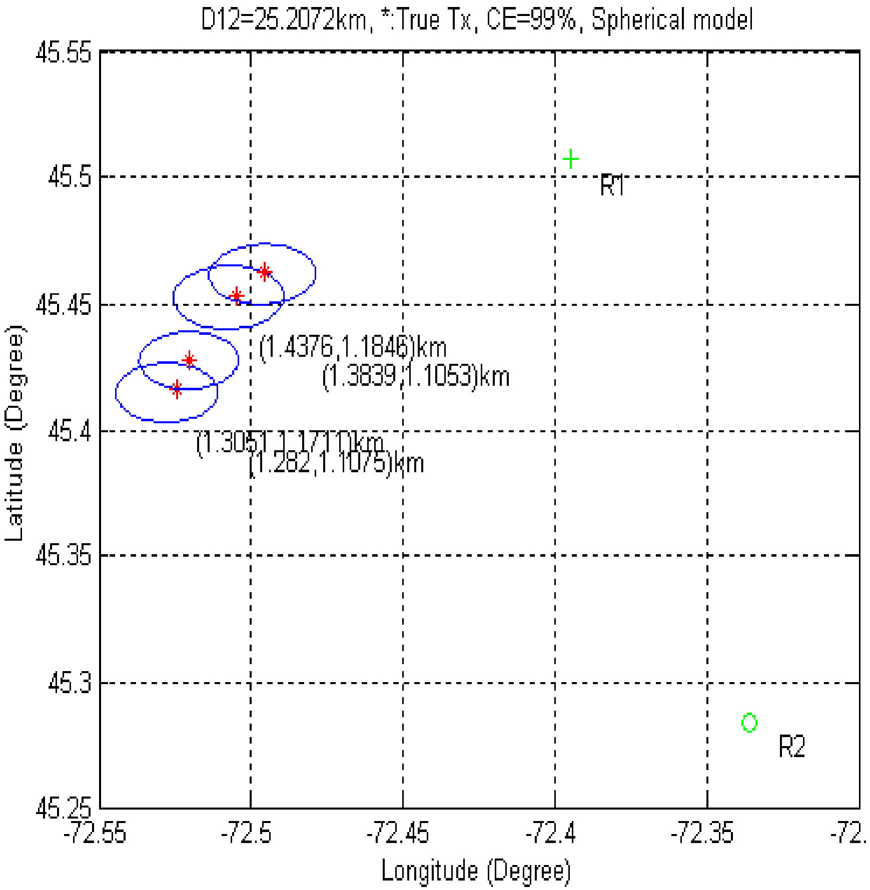

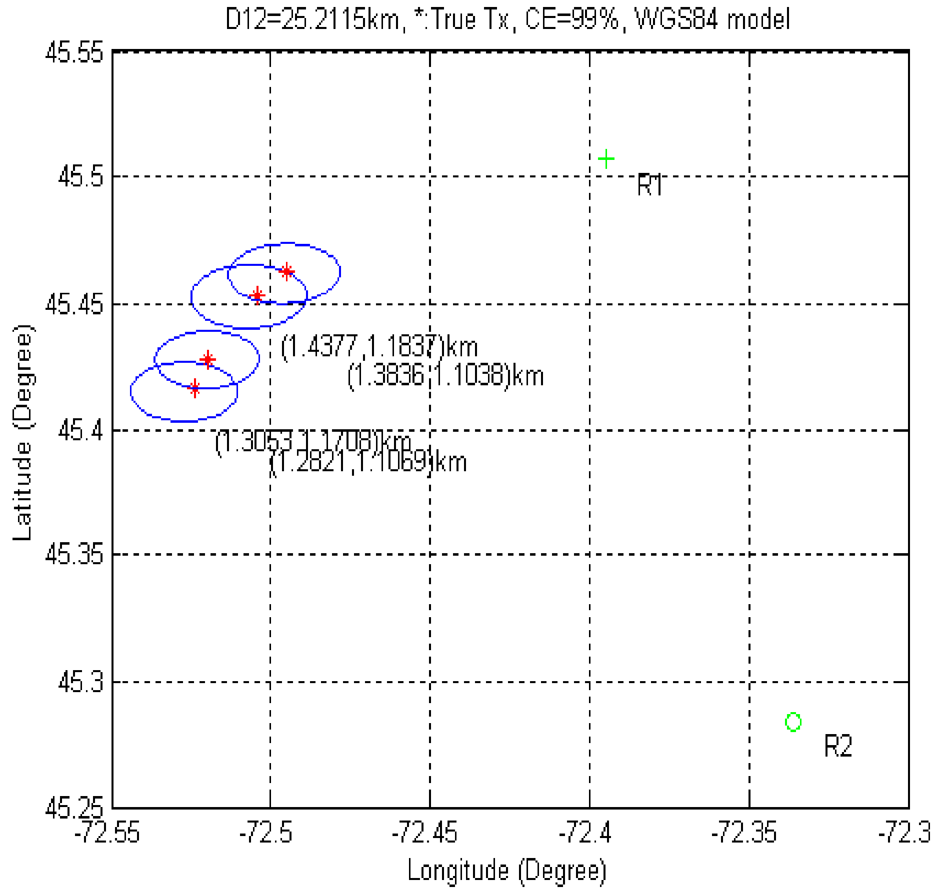

- <u>Simulated Test3 Scenario</u>: Mobile T1&T2 for a 3R fixing with 2-dg AOA SD and *P*=99% CE.

AOA1,2,3_T1(1,2) = (225°,228°),(315°,318°),(90°,93°),
AOA1,2,3_T2(1,2) = (235°,238°),(325°,328°),(80°,83°).

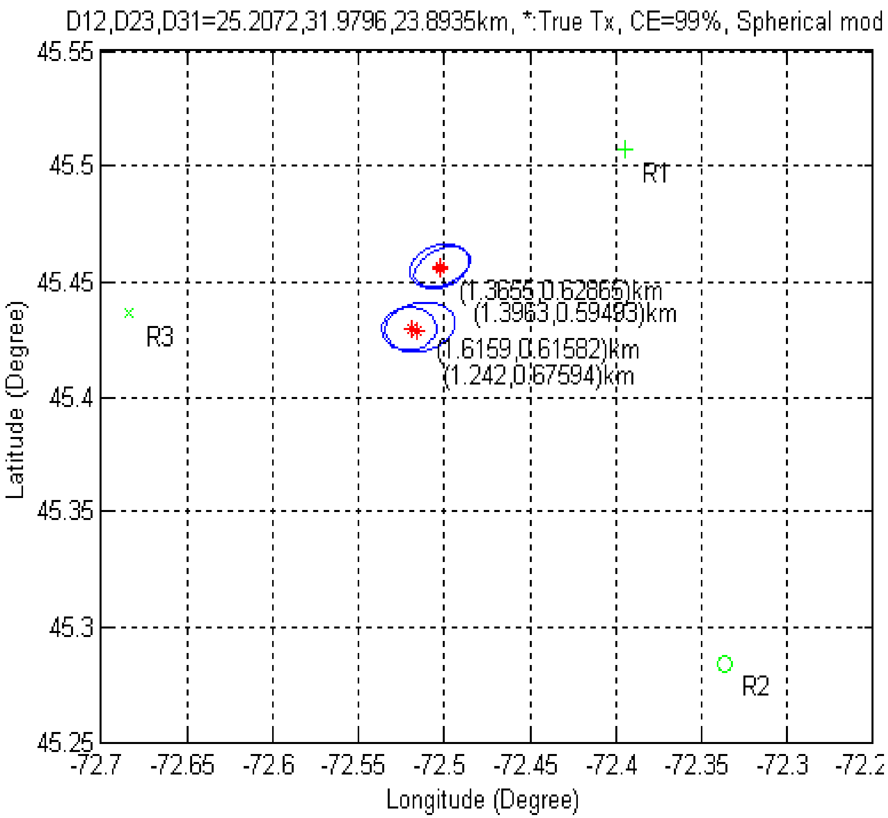

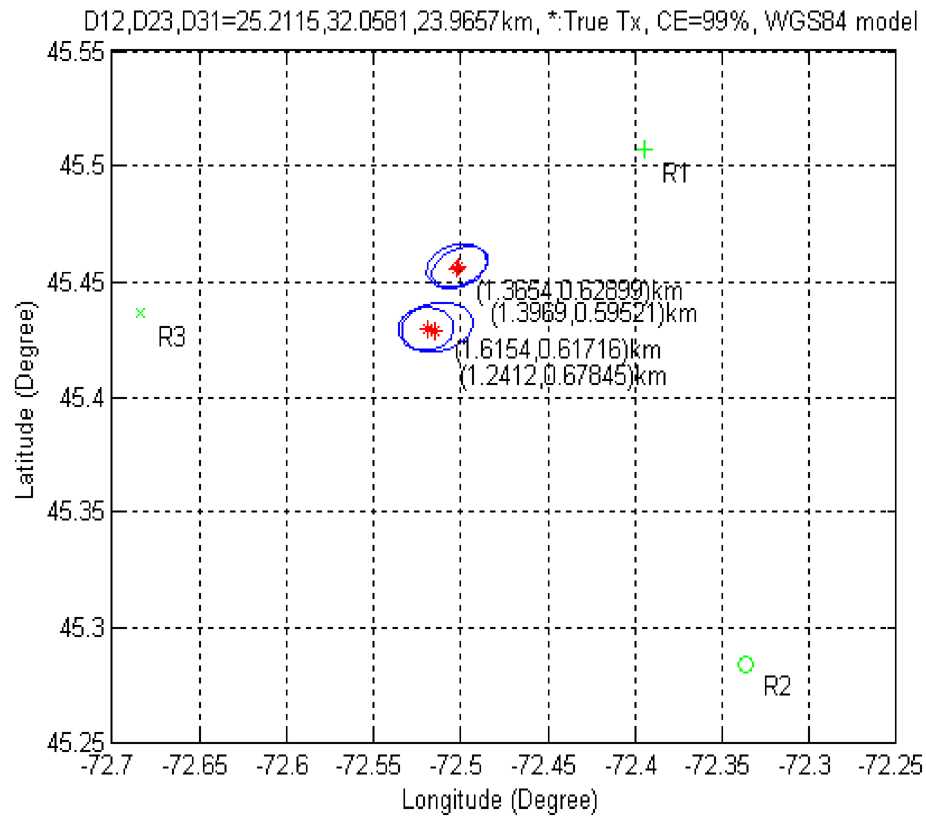

	Spherical	WGS84
Simulated Test1 (I): AOA1=225, AOA2=315 dgs, 1-dg SD, 50% conf.		
Er_AOA1/2_T1(dg)	-0.21141/0.24453	-0.21142/0.24459
True_T1(la_dg,lo_dg)	(45.4162, -72.5244)	(45.4162, -72.5238)
*Vavg*_T1(la_dg,lo_dg)	(45.4164, -72.5231)	(45.4165, -72.5226)
(*r_max*, *s_max*)_T1(km)	(0.28111, 0.23656)	(0.28108, 0.23649)
RMSD_T1(km)	0.38072	0.38077
AREACE_T1 (km^2)	0.20891	0.20883
Simulated Test1 (II): AOA1=225, AOA2=315 dgs, 1-dg SD, 99% conf.		
Er_AOA1/2_T1(dg)	-0.21141/ 0.24453	-0.21142/0.24459
True_T1(la_dg,lo_dg)	(45.4162, -72.5244)	(45.4162, -72.5238)
*Vavg*_T1(la_dg,lo_dg)	(45.4164, -72.5231)	(45.4165, -72.5226)
(*r_max*, *s_max*)_T1(km)	(0.72459, 0.60974)	(0.72451, 0.60957)
RMSD_T1(km)	0.38072	0.38077
AREACE_T1 (km^2)	1.388	1.3874
Simulated Test1 (III): AOA1=225, AOA2=315 dgs, 2-dg SD, 99% conf.		
Er_AOA1/2_T1(dg)	-0.43712/0.49647	-0.43715/0.49652
True_T1(la_dg,lo_dg)	(45.4162, -72.5244)	(45.4162, -72.5238)
*Vavg*_T1(la_dg,lo_dg)	(45.4166, -72.5218)	(45.4167, -72.5212)
(*r_max*, *s_max*)_T1(km)	(1.4536, 1.2345)	(1.4535, 1.2342)
RMSD_T1(km)	0.76158	0.76167
AREACE_T1 (km^2)	5.6374	5.6359

Simulated Test2: AOA1_T1(1,2)=225,228, AOA2_T1(1,2)=315,318, AOA1_T2(1,2)=235,238, AOA2_T2(1,2)=325,328 dgs, 2-dg SD, 99% conf.		
Er_AOA1_T1(1,2)(dg) Er_AOA2_T1(1,2)(dg)	0.32178, -0.047916 -0.80228, -0.040003	0.32177, -0.047892 -0.80221, -0.039927
True_T1(1)(la_dg,lo_dg) True_T1(2)(la_dg,lo_dg)	(45.4162, -72.5244) (45.4277, -72.5205)	(45.4162, -72.5238) (45.4278, -72.5199)
*Vavg*_T1(1)(la_dg,lo_dg) *Vavg*_T1(2)(la_dg,lo_dg)	(45.4148, -72.5277) (45.4275, -72.5205)	(45.4149, -72.5272) (45.4276, -72.52)
(*r_max*, *s_max*)_T1(1)(km) (*r_max*, *s_max*)_T1(2)(km)	(1.3051, 1.1711) (1.282, 1.1075)	(1.3053, 1.1708) (1.2821, 1.1069)
RMSD_T1(1,2)(km)	0.72998/ 0.94992	0.73003/ 0.72995
AREACE_T1(1,2) (km^2)	4.8017/ 4.4606	4.801/ 4.4584
Er_AOA1_T2(1,2)(dg) Er_AOA2_T2(1,2)(dg)	0.41135, -0.47495 -0.48043, -0.29088	0.41132, -0.47493 -0.48038, -0.29083
True_T2(1)(la_dg,lo_dg) True_T2(2)(la_dg,lo_dg)	(45.4531, -72.5048) (45.463, -72.4955)	(45.4531, -72.5043) (45.4631, -72.4951)
*Vavg*_T2(1)(la_dg,lo_dg) *Vavg*_T2(2)(la_dg,lo_dg)	(45.4526, -72.5074) (45.4618, -72.4963)	(45.4527, -72.5069) (45.4619, -72.4958)
(*r_max*, *s_max*)_T2(1)(km) (*r_max*, *s_max*)_T2(2)(km)	(1.4376, 1.1846) (1.3839, 1.1053)	(1.4377, 1.1837) (1.3836, 1.1038)
RMSD_T2(1,2)(km)	0.87361/ 0.78357	0.87379/ 0.87371
AREACE_T2(1,2) (km^2)	5.3501/ 4.8054	5.3463/ 4.798

Simulated Test3: AOA1_T1(1,2)=225,228, AOA2_T1(1,2)=315,318, AOA3_T1(1,2)=90,93, AOA1_T2(1,2)=235,238, AOA2_T2(1,2)=325,328, AOA3_T2(1,2)=80,83 dgs, 2-dg SD, 99% conf.		
Er_AOA1_T1(1,2)(dg) Er_AOA2_T1(1,2)(dg) Er_AOA3_T1(1,2)(dg)	2.4732, 0.68219 4.4999, 0.34127 2.6763, 0.17662	2.459, 0.6615 4.4743, 0.3225 2.6639, 0.15849
True_T1(1)(la_dg,lo_dg) True_T1(2)(la_dg,lo_dg)	(45.4289, -72.5158) (45.4291, -72.5194)	(45.4288, -72.5153) (45.4291, -72.5189)
*Vavg*_T1(1)(la_dg,lo_dg) *Vavg*_T1(2)(la_dg,lo_dg)	(45.4303, -72.5141) (45.4295, -72.5206)	(45.4303, -72.5137) (45.4295, -72.5201)
(*r_max*, *s_max*)_T1(1)(km) (*r_max*, *s_max*)_T1(2)(km)	(1.6159, 0.61582) (1.242, 0.67594)	(1.6154, 0.61716) (1.2412, 0.67845)
RMSD_T1(1,2)(km)	1.4094/ 0.68348	0.87823/ 0.87822
AREACE_T1(1,2) (km^2)	3.1262/ 2.6375	3.132/ 2.6455
Er_AOA1_T2(1,2)(dg) Er_AOA2_T2(1,2)(dg) Er_AOA3_T2(1,2)(dg)	0.81012, -1.657 1.0897, -2.1499 0.89494, -2.2815	0.81611, -1.6443 1.1006, -2.1406 0.90839, -2.2694
True_T2(1)(la_dg,lo_dg) True_T2(2)(la_dg,lo_dg)	(45.4556, -72.5026) (45.4569, -72.5022)	(45.4557, -72.5021) (45.457, -72.5017)
*Vavg*_T2(1)(la_dg,lo_dg) *Vavg*_T2(2)(la_dg,lo_dg)	(45.4564, -72.5013) (45.4566, -72.503)	(45.4565, -72.5008) (45.4567, -72.5025)
(*r_max*, *s_max*)_T2(1)(km) (*r_max*, *s_max*)_T2(2)(km)	(1.3655, 0.62865) (1.3963, 0.59493)	(1.3654, 0.62899) (1.3969, 0.59521)
RMSD_T2(1,2)(km)	0.81975/ 0.95306	0.90192/ 0.90193
AREACE_T2(1,2) (km^2)	2.6968/ 2.6097	2.6981/ 2.612

Observations

- (Er_AOAi_Tj, *Vavg*_Tj, RMSD_Tj) are independent of *P* of CE.
- Higher *P* of CE leads to larger (*r_max*, *s_max*) (i.e.
- AOA SDs are used for *Vavg* and (*r_max*, *s_max*) in the 3R fixing. While AOA SDs are only used for (*r_max*, *s_max*) in the 2R fixing.
- The accuracy of *Vavg* and (*r_max*, *s_max*) should be higher for the 3R fixing with the extra information from the third RX.
- 2R AREACE is generally larger than its 3R counterpart.
- At a certain *P* of CE, a smaller CE indicates a more accurate estimate of a TX's location. Thus, with higher accuracy of *Vavg*, (*r_max*, *s_max*), and smaller AREACE, the 3R fixing can locate the TXs better than the 2R fixing with the tradeoff that one more RX is needed.
- Spherical and WGS84 results are close to each other in this study.

Some limitations

- (Stansfield): For 2R fixing, to have adequate reliability, AT1 should be at least 30 dgs.
- Larger AOA SD and RX-TX arc distance *S* lead to larger CE (i.e. CE (i.e. worse location estimation)=>some limitations for D and *S*.

  since $\sigma_{\psi J}$ >Bessel)≈ $\sigma_{\psi J}$

  o large. A separated 2R fixing simulation to test *P* of CE showed that it at it is reliable when AOA SD < 4 dgs with (*S*_R1T1, *S*_R2T1, *S*_R1R2) ~ _R1R2) ~ (22,11,25) km.

  ,25) km.

Conclusions and Future Study

- The results demonstrated the effectiveness of using both geodetic models to track mobile TXs in a 2R/3R fixing.
- The 3R fixing can locate the TXs better than the 2R fixing, with the tradeoff being that one more RX is needed.
- The results from Spherical and WGS84 models are close to each other.
- Actually measured data for a 2R/3R fixing with mobile TXs will be used to test the capability of the algorithms in this study.
- The equations for large AOA SD without approximations will be derived if they are needed for measured cases.
- The cases for *S* longer than 50 km will be investigated.